



ACADEMIC
PRESS

Available online at www.sciencedirect.com

SCIENCE @ DIRECT®

NeuroImage

NeuroImage 19 (2003) 1061–1075

www.elsevier.com/locate/ynimg

Magnetoencephalographic evidence of the interhemispheric asymmetry in echoic memory lifetime and its dependence on handedness and gender

Andreas A. Ioannides,^{a,*} Mihai Popescu,^a Asuka Otsuka,^a Anastasios Bezerianos,^b and Lichan Liu^a

^a *Laboratory for Human Brain Dynamics, RIKEN Brain Science Institute, 2-1 Hirosawa, Wako-shi, Saitama, 351-0198, Japan*

^b *Medical Physics Department, School of Medicine, University of Patras, Patras 26500, Greece*

Received 6 November 2002; revised 21 February 2003; accepted 20 March 2003

Abstract

The echoic memory trace (EMT) refers to neuronal activity associated with the short-term retention of stimulus-related information, especially within the primary and association auditory cortex. Using magnetoencephalography it is possible to determine quantitatively the lifetime of the EMT. Previous studies assumed that each new stimulus drives the EMT to its full strength, which then passively decays. In this study we show the limitations of this assumption using trains of auditory stimuli designed specifically for computing the EMT lifetime and its contextual sensitivity. We estimated a time-dependent EMT using a data-driven approach, which allows contributions from a relatively wide area around the auditory cortex in our quantitative measures. We identified: (1) internally generated cortical activations during the silent period between stimuli well separated in time from each other, which had influence on the morphology of the neuromagnetic response to the next external stimulus; and (2) EMTs with different lifetimes that modulate the amplitude of the evoked responses at different latencies, suggesting the existence of multiple neural delay lines. Long EMT lifetimes were observed on the descending part of the M100 complex, which showed handedness and gender-dependent interhemispheric asymmetry. Specifically, all subjects showed longer EMT lifetimes on the left hemisphere, except left-handed males. Distributed source analysis of the data for one left- and one right-handed male subject identified a secondary generator in the right-handed subject, which was located posterior to the early primary generator and dominated the auditory response at late latencies, where EMT lifetime asymmetry was high. The identified multiple neural delay lines and their laterality may provide a link between macroneuronal activity and left hemisphere specialization for processing linguistic material.

© 2003 Elsevier Science (USA). All rights reserved.

Introduction

Stimulation of sense organs induces a modality-specific neural representation, which has a brief but nevertheless finite duration. The echoic memory trace (EMT) is the activity in primary and association auditory cortical areas related to the retention of stimulus features, which persists for some time after the stimulus presentation. The EMT is necessary for integrating successive perceptual features whenever acoustic information is continuously presented,

such as continuous speech or melody. Meaningful analysis of any acoustic transient requires more than just an analysis of its physical properties. Saliency depends on context and novelty, which can only be evaluated if a prolonged neural representation of previous events is available, as either a persistent network state or a specific decaying activity pattern (Bugmann and Taylor, 1997; Bugmann, 1997). Neural models based on exponentially decaying memory processes provided good accounts for the data from temporal duration discrimination tasks (Wearden, 1992) and were consistent with the stochastic nature of biological timing (Grossberg and Merrill, 1992, 1996). By definition, EMT relates to neuronal responses to auditory stimuli, but at what level this

* Corresponding author. Fax: +81-48-467-9731.

E-mail address: ioannides@postman.riken.go.jp (A.A. Ioannides).

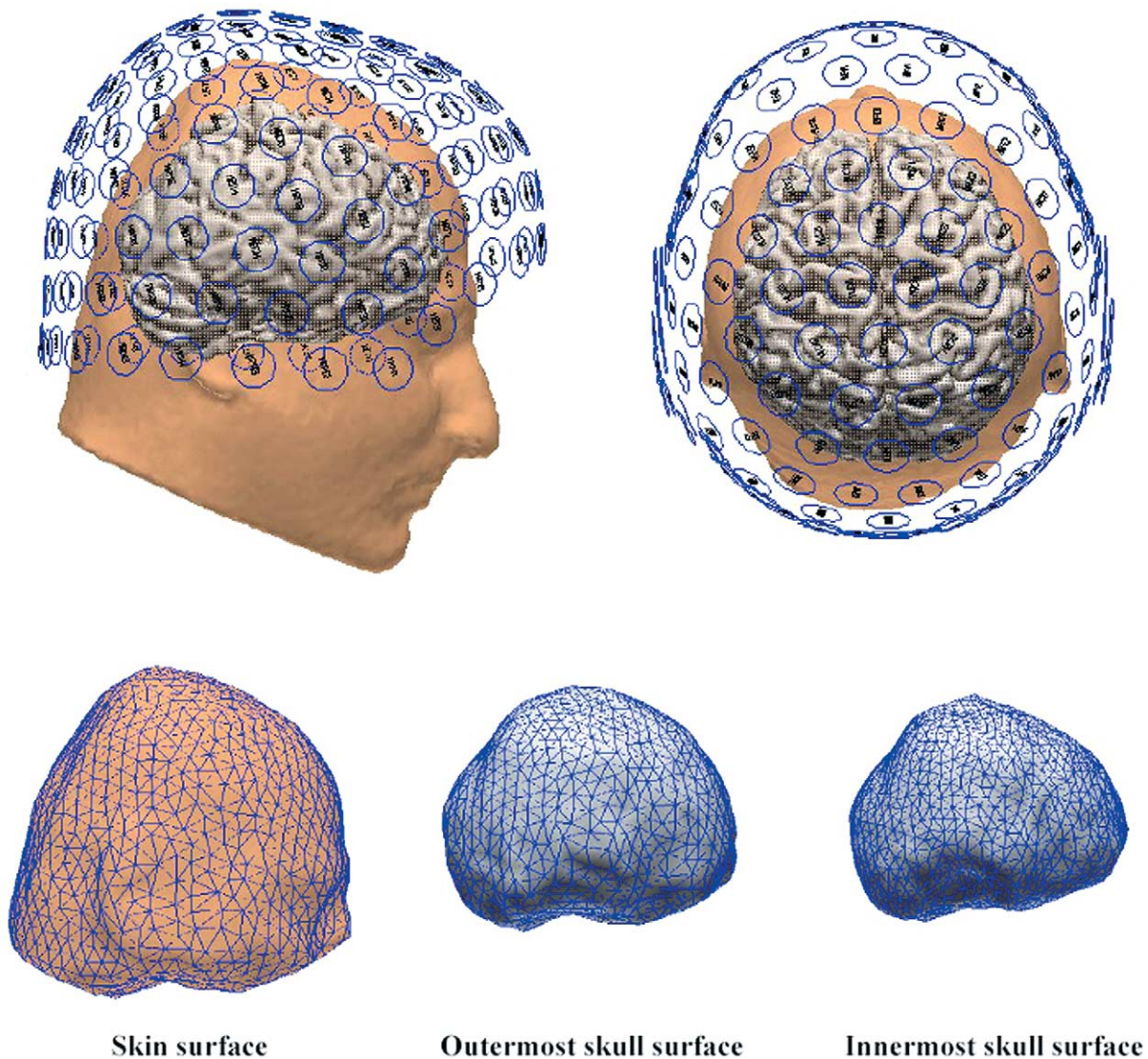
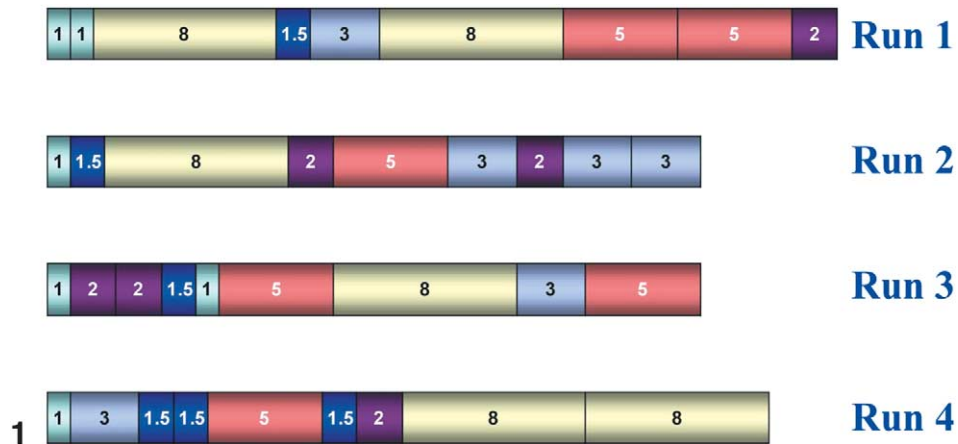
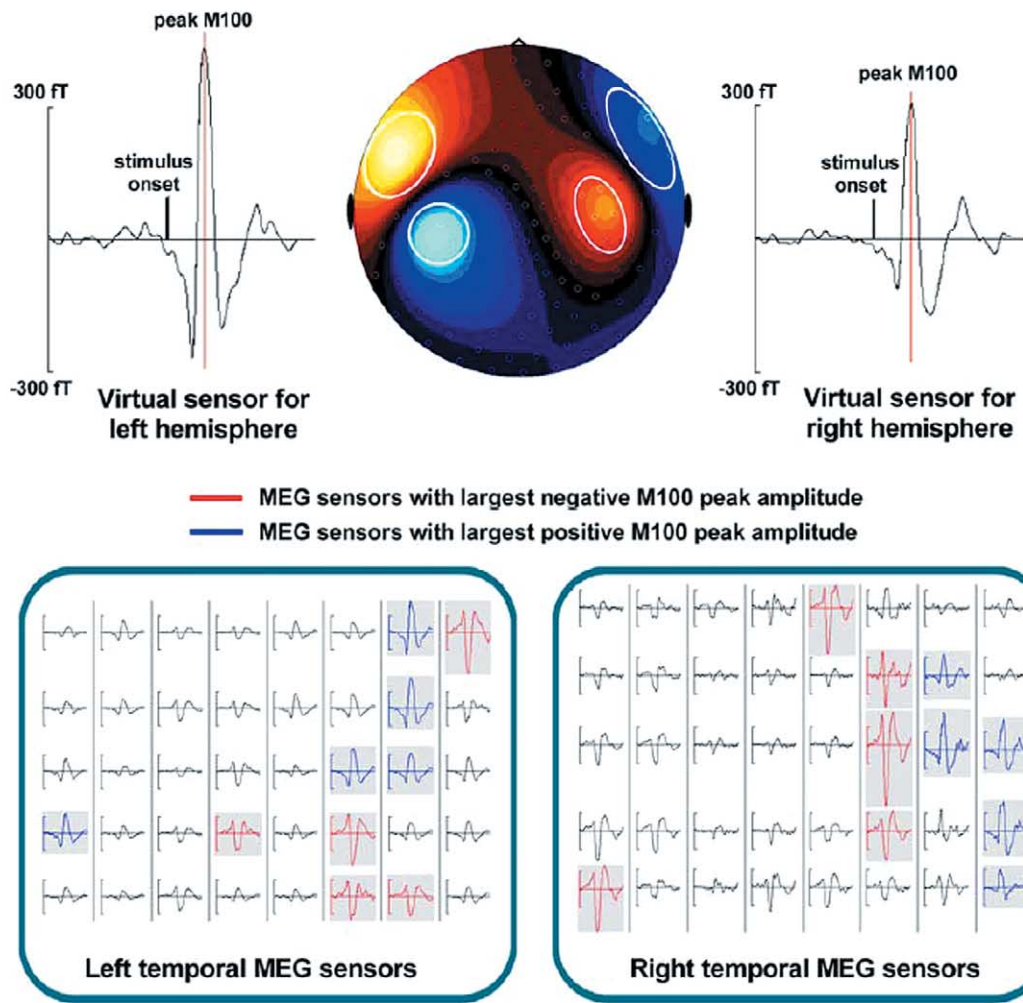


Fig. 1. Design of stimuli sequences. The tones were delivered in four separate runs, each containing 30 repetitions of a 9-tone block. Within each block, tones were spaced in a fixed sequence using 6 preselected ISI values (1, 1.5, 2, 3, 5, and 8 s). Distinct colors in the figure are associated with each of these ISI values. The first ISI of each block follows the last ISI of the previous block. The design of the ISI sequences ensures that different histories have equal contributions to the averaged responses (each ISI is once and only once preceded by each of the ISIs in the preestablished list, as emphasized by the color code used in the illustration).

Fig. 3. Example of head and brain surfaces segmented from MRI data. (Top row) Skin and brain surfaces and the sensor set-up for MEG measurements (left panel: right side view; right panel: top view). (Bottom row) The three brain compartments of the volume conductor BEM model: skin (10 mm mean triangle edge length), outside skull (9 mm mean triangle edge length), and inside skull (liquor brain compartment, 7 mm mean triangle edge length).

A. Channel selection for Virtual Sensor computation.



B. Sensitivity profile of the Virtual Sensor

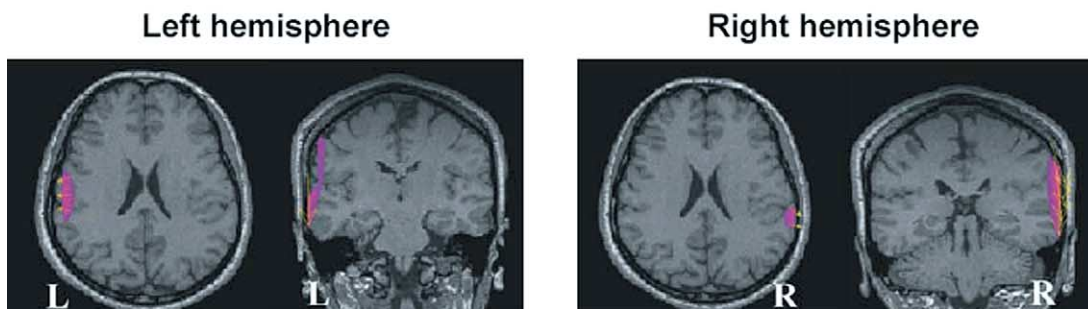


Fig. 2. Virtual sensor definition. (A) Channel selection for virtual sensor computation. The virtual sensor signal is separately computed for each hemisphere as a linear combination of the channels showing the largest positive and negative peak amplitude at the M100 latency, marked in blue and red, respectively. (B) The overall sensitivity of the left and right hemisphere VS for one subject. The weights of the VS are chosen directly from the signal over the left and right temporal cortex at the M100 peak. The overall sensitivity of the VS is simply the weighted sum of the lead fields (vector sensitivity profile) of each sensor. The red region marks the region with VS sensitivity modulus above 70% of the maximum, while the thin yellow arrows show the local direction of the sensitivity profile.

relationship should be established is not clear. Recent studies to be reviewed below suggest that the EMT properties can be usefully studied at the level of macroelectrophysiology accessible to magnetoencephalography (MEG) and EEG, and especially in terms of the way the response varies with the time between successive stimuli.

Early pioneering investigations using passive listening to simple tones separated by constant silent intervals related the EMT to the dependence of the N100/M100 peak amplitude on the time between successive stimulus presentations. For consistency with these earlier studies we will use henceforth the term interstimulus interval (ISI) to refer to the *onset-to-onset* time interval between consecutive stimuli. A qualitative increase in the evoked response with the increase of ISI was identified in both electric (Celesia, 1976) and magnetic (Hari et al., 1982, 1987) recordings and referred to as *temporal recovery function*. The data and analysis did not distinguish whether the effect was due to loss of excitability or increase of inhibition, or whether the mechanism was cortical. The exponentially decaying EMT model proposed later (Lü et al., 1992a, 1992b) produced similar lifetimes across the two hemispheres that varied markedly across subjects, but were consistently higher in the association cortex than the primary cortex. In these studies, the estimates of either a single EMT lifetime or one EMT lifetime in the primary and one in the association auditory cortices used only the value of the average signal at one latency, corresponding to either the peak signal or the peak strength of the equivalent current dipole. Such analysis implies that a unitary cortical response in a given area is driven to its full strength by each tone and then decays passively and uniformly with time thereafter. In this work, we have relaxed this assumption by allowing for the processing of acoustic stimuli by distinct sets of neuronal pools, each having its own characteristic activation pattern with distinct peak latency and EMT lifetime.

After the onset of an auditory stimulus, many cortical areas are excited over a wide area around the primary auditory cortex well within 100 ms. Direct evidence from intracranial recordings shows further that an omitted stimulus in an otherwise regular train of stimuli excites some of the same areas at about the same latencies (Hughes et al., 2001), so the context within which a stimulus is presented influences the response. In this work, we considered that the evoked response depends on both the time interval to the last stimulus and internal and external context. We defined the history of previous stimuli as external context and the history of brain activations as internal context, which related more to the state of the subject rather than to direct responses evoked by stimuli. We used sequences of stimuli with varying ISI (Fig. 1) to study the context sensitivity. If the EMT lifetime depends on external (stimulus-related) context and not just on the ISI of the last stimulus, then the previous history of stimulation will influence the EMT. We designed our stimulus sequence so that the dependence of EMT lifetime on the previous history could be reliably

modeled for the last two ISIs within a sequence of different ISIs. Internal context will manifest itself as changes of the response to a stimulus modulated by brain activity, which is not directly elicited by any of the stimuli. In general such activations may occur anywhere in the brain and influence the EMT. We restricted our investigation to internally generated activations that showed a direct influence on the morphology of the auditory response evoked by external stimuli.

A description of EMT in terms of purely localized activity is unlikely to be realistic. The neuronal implementation of sustained activity is likely to involve local and distant connections with multiple delay lines (Miller, 1996). Some of the converging impulses may indeed lead to localized activations, especially for early responses within or close to the primary auditory cortex. It is not, however, necessary that these responses will remain localized to one or a few foci. In dealing with this problem we used an analysis that does not rely on focal activation, but rather is driven by the major features of the signal distribution to identify the major classes of phenomena related to the EMT. By limiting precision over unknown properties (number and location of generators) and allowing more flexibility in the form of the EMT we were able to identify laterality effects which are very likely related to the different way the two hemispheres deal with linguistic material.

Early studies documented well the left hemisphere dominance in speech and language for right-handed humans, but they tended to overemphasize the role of areas on the left superior temporal lobe, without convincing physiological explanations (Luria, 1970; Wernicke, 1977). Related research conducted on lesioned epileptic patients made a step forward and linked the handedness with language lateralization, estimating that left-hemisphere language dominance occurred in 96% of dextrals and 70% of sinistrals (Rasmussen and Milner, 1977). Nevertheless, equally distributed speech response cells have been identified in the middle area of the superior temporal gyrus in both hemispheres (Creutzfeldt et al., 1989) and the isolated right hemisphere of dextrals has been proved to perceive syntactically simple spoken sequences (McGlone, 1984; Zaidel, 1985). These observations led to the flexible hypothesis that *both* hemispheres provide routes to speech perception (Hickok and Poeppel, 2000), but with preference of the route from the *left* hemisphere under normal conditions (Boatman et al., 1998). Hence, lateralization might have been selected over bilateral representation because it improves the temporal accuracy of sequential processing of the incoming stream of acoustical events, by removing unnecessary delays imposed by the relatively slow interhemispheric pathways (Ringo et al., 1994; Corballis, 1998). This hypothesis is supported by recent findings showing that temporal coding is preferentially processed in the left auditory cortex, and appears to offer the most plausible advantage for language lateralization (Robin et al., 1990; Liegeois-Chauvel et al., 1999). Our results reveal an

interhemispheric asymmetry of the EMT lifetime and a handedness–gender interaction. This rather surprising result is nevertheless in line with recent findings using imaging (Gur et al., 1982) and anatomical (Amunts et al., 2000) techniques and in agreement with the well-known “testosterone hypothesis” (Geschwind and Galaburda, 1987).

Materials and methods

Subjects and stimuli

The CTF whole head OMEGA system (151 axial gradiometers) was used to record MEG signals from 24 subjects: 12 right-handed (6 males) and 12 left-handed (6 males), with no history of otological or neurological disorders and normal audiological status (air conduction threshold no more than 10 dB hearing level). Handedness was estimated using the Edinburgh Handedness Inventory (Oldfield, 1971). The experiment and its goals were described to the subjects before they gave their informed consent to participate. The subjects were instructed to listen passively to auditory tones presented binaurally in four runs. The tones were delivered using echo-free plastic tubes. Each tone (1 kHz, 60 dB nHL) had a duration of 200 ms (rise and fall times of 10 ms). Each run contained 30 repetitions of a block of stimuli. In each block, 9 tones were spaced in a fixed sequence using 6 ISI values (1, 1.5, 2, 3, 5, and 8 s). If the EMT lifetime depends on external (stimulus-related) context and not just the ISI of the last stimulus, then many previous stimuli should in theory be modeled. However, since the EMT decay is relatively fast, retaining few terms should be a good approximation for stimuli with fairly long ISIs. This is also supported by the results of the EMT lifetime estimation for blocked and interleaved presentation of stimuli with different ISIs (Liu et al., 1998a). The stimulus sequences were designed so that the dependence of the EMT lifetime on the last two ISIs could be studied. The onset-to-onset latency difference between the current stimulus and the previous one is labeled as *target* ISI. The onset-to-onset latency difference between the previous and the one before stimuli is labeled as *contextual* ISI since it approximates the stimulation history before the previous stimulus. The sequences in the blocks were designed to allow the cross-averaging of the responses following the same target (first preceding) ISI but with equiprobable presentation of a different history of the contextual (second preceding) ISI. We denote by $s_{x|y}^n$ the evoked response elicited by a tone, which belongs to the n th block of a run,

preceded by an interstimulus interval x and conditioned by a contextual (second preceding) interstimulus interval y . This allows us to define the intra-run subaveraged response $\bar{s}_{x|y}$ as:

$$\bar{s}_{x|y} = \frac{1}{N} \sum_{n=1}^N s_{x|y}^n, \quad N = 30.$$

The cross-averaged (inter-run) response to a first preceding ISI x is simply defined by:

$$\bar{s}_x = \frac{1}{M} \sum_y \bar{s}_{x|y}, \quad M = 6.$$

The design of the ISI sequences ensures that different histories have equal contributions to the cross-averaged signals (each target ISI is once and only once preceded by each of the contextual ISI values). To avoid learning of the block sequences by the subjects, we used the passive listening paradigm and short duration of each run. The short duration of each run was also used to ensure reasonable alertness level and to limit the subjects' head movement during the recording.

Virtual sensor computation

The early peaks in the average MEG signal elicited by auditory stimuli, particularly the M100, have predominantly dipolar distributions. A weighted average can be defined around each channel i as below:

$$VS_i(t) = \sum_{j=1}^N \exp\left[-\left(\frac{|\mathbf{r}_j - \mathbf{r}_i|}{\lambda}\right)^2\right] \cdot s_j(t),$$

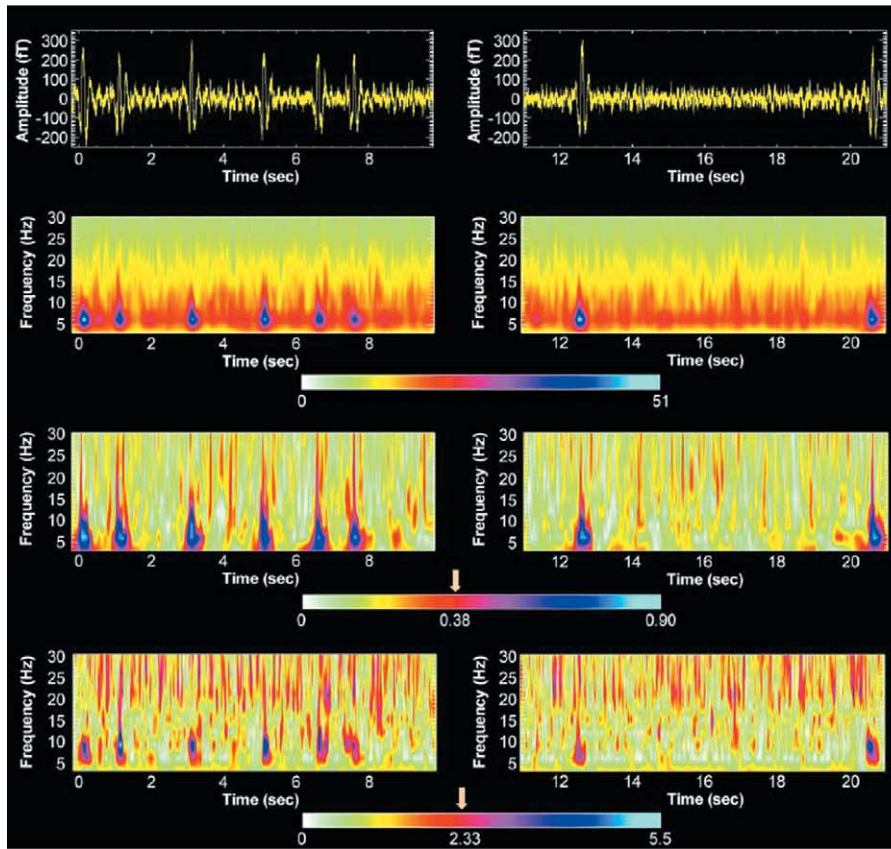
where λ is the characteristic length and s_j is the MEG signal measured by channel j , at the position vector \mathbf{r}_j . This smoothing operation minimizes noisy contributions and can be applied separately to the extrema of the dipolar pattern (Liu et al., 1998b). Even more simply, the five channels (k_1 to k_5) that produced the most clear positive deflections and the five channels (p_1 to p_5) that produced the most clear negative deflections at the time of the M100 peak can be selected to define the composite virtual sensor signal (henceforth referred to as VS):

$$VS(t) = \frac{1}{5} \left[\sum_{i=1}^5 VS_{k_i}(t) - \sum_{i=1}^5 VS_{p_i}(t) \right].$$

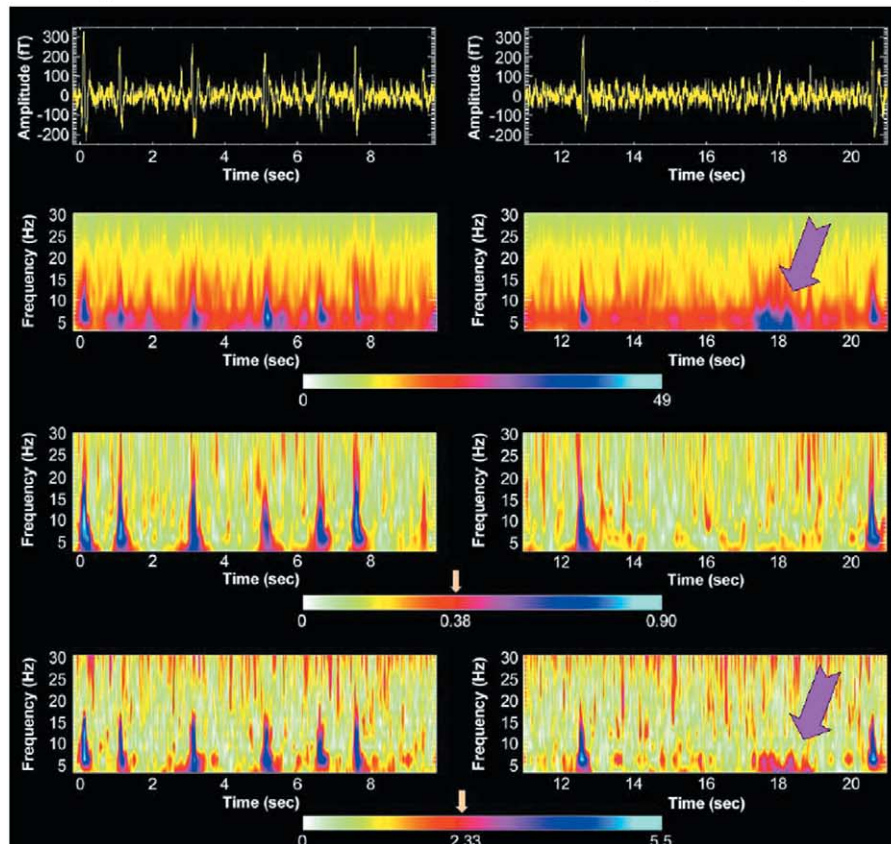
The choice of sensors is made directly from the field maps at the time of the peak activity, as shown in Fig. 2A. Using

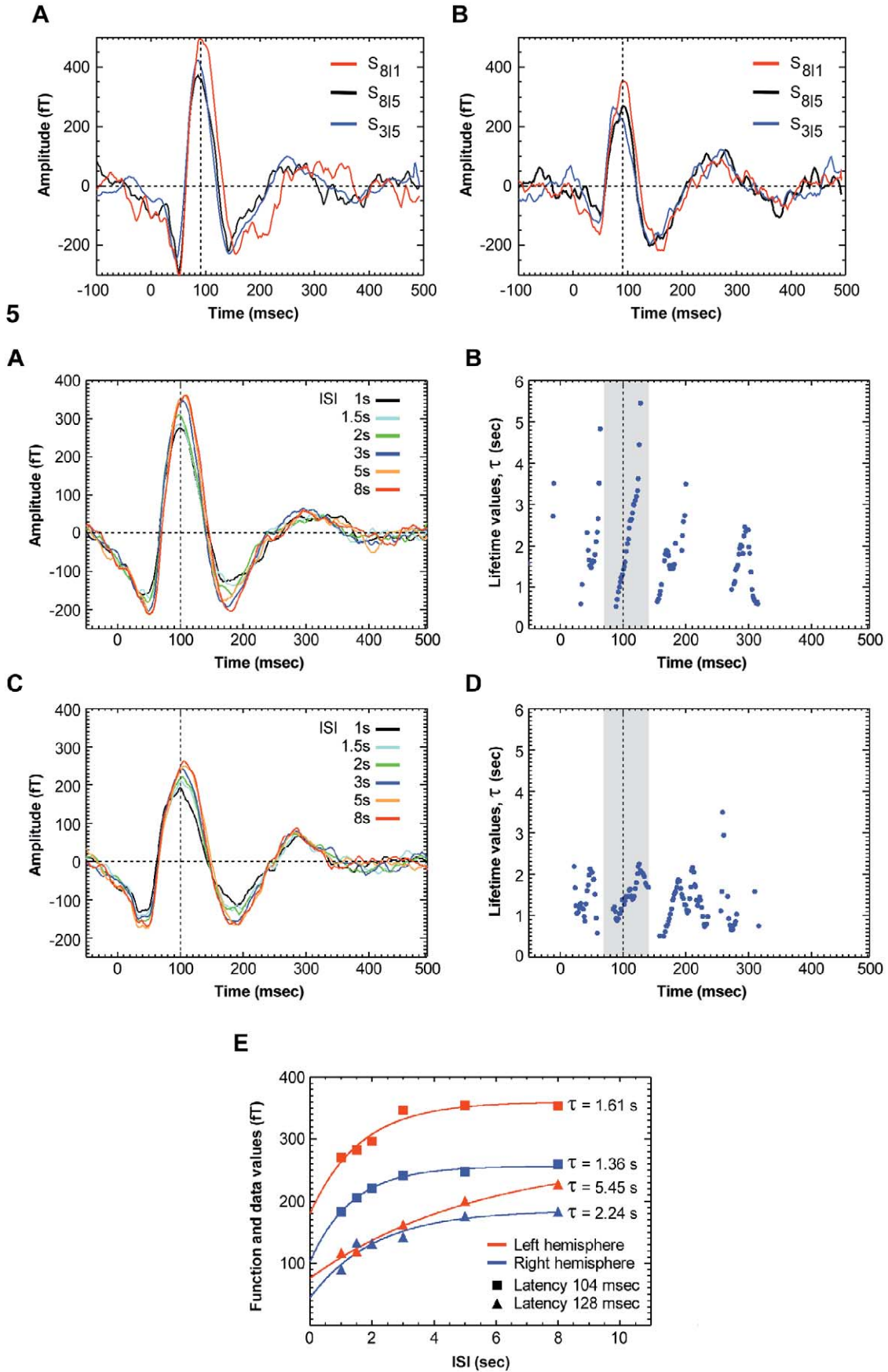
Fig. 4. Examples of time-locked and non-time-locked activity. The rows illustrate segments extracted from the averaged VS signal (first), and the corresponding averaged scalograms (second), phase-ordering factors (third), and Z score maps (fourth). The panels in the left column correspond to a segment of consecutive short ISIs, while the panels in the right column illustrate a segment with a long ISI (both segments were extracted from the third run of the experiment). The arrows on the color bar corresponding to the POF and Z score maps indicate the threshold of statistical significance ($P < 0.01$). (A) Subject S1, right hemisphere. (B) Subject S20, right hemisphere. The clearest NTLA is indicated by heavy arrows, on the averaged scalogram and Z score map.

A. Subject S1: NTLA is not detected.



B. Subject S20: clear NTLA is detected on long silent segments.





five (rather than one) sensors in each of the two subsets ensures that the compound signal from generators between the two sets of sensors is picked up almost evenly. The same set of sensors remains close to the optimal for earlier or later latencies in the period we have studied. The spatial sensitivity profile of the VS (Fig. 2B) is broadly, but not exclusively, focused on the auditory cortex (Liu et al., 1998b), but it is considerably sharper than the very poor spatial sensitivity profile of each sensor. It is sufficiently broad to allow for contributions from extended regions or nearby foci that might be activated at different latencies and/or in different single trials. Activity from generators in or close to the primary auditory cortex will contribute with one sign (say positive) to neuromagnetometers located over the parietal area of the scalp and with the opposite sign (negative) to neuromagnetometers over the anterior temporal area. A latency dependence in the VS output can be generated by either activity variations in spatially overlapping neuronal pools or changes in relative strength in nearby but spatially separated generators within the VS region of sensitivity. The choice of VS for the analysis was made to match the requirements of the study. The computational efficiency of VS was an added bonus, which allowed us to follow the activity in the auditory cortex with good efficiency over the entire period and not just at the M100 peak.

Data fitting

The continuous data stream in each virtual sensor signal was divided into 700-ms segments, each beginning 200 ms before stimulus onset. A four sample (6.4 ms) moving average was used to smooth out the small remaining high-frequency fluctuations. The signal was further processed at latencies with significant and consistent activation, selected on the basis of the following simple rule: the signals following different ISIs must be either all positive or all negative. At these latencies, the least-square best-fit estimate has been computed by implementing a gradient steepest descent algorithm for a three-parameter model:

$$A(1 - e^{(t_0 - \text{ISI})/\tau}),$$

where A is the amplitude, t_0 is the intercept or time of decay onset, and τ is the lifetime. The fitting criteria were further restricted demanding that convergence of the fitting algorithm to a tolerance of 0.001 is achieved within 10 itera-

Table 1
Summary of the lifetime (τ) values and asymmetry coefficients

Subject	Gender (M/F)	Handedness (RH/LH)/laterality quotient (%)	τ values (s)				Asymmetry coefficient (%)
			τ values at latency \bar{L}_{M100}		Maximal τ values (s)		
			Left	Right	Left	Right	
S 1	M	RH/100	1.6	1.4	5.5	2.2	43
S 2	M	RH/100	1.0	0.8	5.1	2.9	28
S 3	M	RH/90	0.9	0.8	5.2	3.6	18
S 4*	M	RH/50	0.9	0.6	4.5	1.0	64
S 5**	M	RH/50	1.5	1.2	4.1	2.5	24
S 6**	M	RH/40	2.4	1.8	4.7	2.9	24
S 7	F	RH/100	1.0	0.7	6.0	1.1	69
S 8**	F	RH/100	1.3	0.9	5.2	3.1	25
S 9**	F	RH/100	1.2	0.9	4.4	2.2	33
S 10*	F	RH/100	1.3	1.1	5.1	2.6	32
S 11	F	RH/100	1.3	0.6	5.5	2.7	32
S 12*	F	RH/58	2.0	1.7	4.4	2.9	21
S 13*	M	LH/100	1.1	0.7	3.00	4.1	-15
S 14	M	LH/75	2.7	3.5	4.6	5.5	-9
S 15	M	LH/50	1.5	1.1	5.8	4.3	15
S 16*	M	LH/30	1.8	1.3	2.9	3.0	-2
S 17	M	LH/50	0.6	0.5	3.4	3.4	0
S 18*	M	LH/80	2.5	2.2	4.7	5.4	-7
S 19*	F	LH/100	2.3	2.6	7.8	4.4	28
S 20*	F	LH/80	1.1	1.3	3.7	1.9	32
S 21	F	LH/70	1.2	0.8	5.7	3.2	29
S 22	F	LH/70	1.5	0.6	4.6	1.1	61
S 23*	F	LH/64	3.4	1.9	6.0	4.1	19
S 24	F	LH/30	1.4	1.7	4.4	2.2	33

Note. The table shows the τ at the mean M100 latency (\bar{L}_{M100}) and the maximal τ value in the temporal window between 70 and 140 ms.

* Fitting was performed after excluding the averaged signals at ISI = 8 s.

** Fitting was performed after excluding the averaged signals at ISI = 5 s and ISI = 8 s.

tions. The goodness-of-fit has also been visually assessed at each latency that passed the previous criteria. It should be stressed that the lifetime parameter alone describes completely the *shape* of the model function: a low lifetime value indicates a sharp decay of the EMT, while a high lifetime parameter indicates a slow decay rate, or a longer persistence of the EMT.

Asymmetry coefficients (AC) on the EMT maximal lifetime values were computed for each subject as:

$$AC = \frac{\tau_{\max}^{\text{left}} - \tau_{\max}^{\text{right}}}{\tau_{\max}^{\text{left}} + \tau_{\max}^{\text{right}}} \times 100 (\%),$$

Fig. 5. NTLA influence on the next response to an external stimulus. The traces in each panel are two responses following target ISIs of 8 s ($s_{8|5}$ and $s_{8|1}$) and one response with combined target and contextual ISI of nearly 8 s. Only the $s_{8|5}$ trace was preceded by high NTLA (in both hemispheres). Although $s_{8|5}$ and $s_{8|1}$ have the same target ISI value, the overall amplitude is decreased more in $s_{8|5}$. The signal is from subject S20 (female, left-handed), whose NTLA is displayed in figure 4B. The $s_{8|5}$ response resembles the response with combined target and contextual ISI of nearly 8 s, suggesting that NTLA produces a similar effect as a veridical response to an external stimulus occurring at the time of NTLA. (A) Signals from the left hemisphere. (B) Signals from the right hemisphere.

Fig. 6. Example of EMT lifetime estimation for one right-handed subject (S1). (A) Evoked responses at different ISIs (left hemisphere). (B) Lifetime of the echoic memory versus latency (left hemisphere). (C) Evoked responses at different ISIs (right hemisphere). (D) Lifetime of the echoic memory versus latency (right hemisphere). (E) Curve fitting at latencies 104 ms (M100 peak) and 128 ms (corresponding to the maximal lifetime values).

where $\tau_{\max}^{\text{left}}$ and $\tau_{\max}^{\text{right}}$ are the maximal lifetime values in a time window between 70 and 140 ms for the left and right hemispheres, respectively.

Wavelet analysis

The Pseudo-Continuous Wavelet Transform (PCWT; Vetterli, 1995) decomposes a signal into a set of time sequences distributed in different frequency bands across the time-frequency plane, by convolution with dilated and translated versions of a mother wavelet. Each single block (trial) signal was convoluted by a Morlet wavelet (complex conjugated gaussian function). The Morlet wavelet was selected because it is defined by an explicit, easy to compute function, and it is based on the Gaussian window, which is the best compromise for the time and frequency resolutions. Furthermore, it allows complete flexibility in setting the PCWT to have a desired frequency resolution at any particular frequency. The wavelet family used in the present study had a temporal resolution of 400 ms at 3 Hz and 40 ms at 30 Hz, and a bandwidth of 1 Hz at 3 Hz and of 10 Hz at 30 Hz. The resulting spectrotemporal map (scalogram) preserves information about both the latency and frequency of the transient signal components. Specifically, we computed the averaged scalograms in conjunction with phase-ordering factors (POFs) and time-frequency maps of Z scores extracted from PCWT. A scalogram derived from the average VS signal provides information about time-locked activations that survive the averaging process. The average of single trial scalograms preserves both time-locked and non-time-locked contributions to the single trial VS signal. A nonparametric sign test was used to assign statistical significance of non-time-locked activations (NTLA) for each time-frequency interval over a selected time period in the stimulation sequence. The POF, which refines the phase averaging in frequency domain (Jervis et al., 1983), was used to estimate the phase distribution of the VS components and its statistical significance. The POF is independent of the signal amplitude and provides information about the time locking of the significant activations revealed by the averaged scalogram.

The time-frequency energy was compared for each single trial with its median value in the baseline, computed from 5-s recordings at the beginning of each run. The Z value was defined at each time-frequency point as follows:

$$Z(t, f_0) = \frac{N^+(t, f_0) - 0.5N}{0.5\sqrt{N}},$$

where $N^+(t, f_0)$ denotes the number of single trials with energy $E(t, f_0)$ above the baseline median value, and N is the total number of single trials. Tabulated probability values indicate that $P < 0.01$ when $Z(t, f_0) > 2.33$. A statistical Rayleigh test was employed in order to check the uniformity of the angle distribution on the unit circle. For 30 single trials (blocks in each run), critical Rayleigh values indicate

that the 0.01 error level corresponds to phase ordering factors greater than 0.387.

To address the question of how the NTLA affect the morphology of the immediately following response to a tone, we have compared the subaveraged signal $s_{x|y}$ (x accounts for the target ISI, while y accounts for the contextual ISI), which is preceded by a consistent self-excitation having a peak wavelet energy localized at Δt before the stimulus onset, with the responses $s_{\Delta t + \varepsilon_1 | x - \Delta t - \varepsilon_2}$, where ε_1 and ε_2 allow for the weak time-locking of the self-excitations. Both values $\Delta t + \varepsilon_1$ and $x - \Delta t - \varepsilon_2$ must be equal to some of the ISI values used in our experiment and as close as possible to the values Δt and $x - \Delta t$, respectively. To achieve the last criterion, the absolute values of the jitters were restricted by:

$$|\varepsilon_1| + |\varepsilon_2| < 1 \text{ s.}$$

Two aspects of this analysis must be clearly stated: first, such a comparison became possible only in cases when both $x - \Delta t$ and Δt are close to some of the pre-established ISI values used in our experiment; second, in some of these cases there were two candidate signals that can meet the above criteria—one of these cases will indeed be described in the following sections.

Co-registration with anatomical MRI scans

The subject's head position relative to the MEG sensors was determined by the localization of the center coordinates of three orthogonal coils fixed on the subject's skin at nasion, left, and right preauricular positions. Since the main analysis of the data was planned with virtual sensors, only a rough outline of the head was obtained for the majority of subjects using the Polhemus FASTRAK 3D Digitizer (Polhemus Inc., Colchester, VT). For a small subset of subjects a complete headshape outline was collected to allow accurate surface matching with the segmented skin surface from MRI data. For subjects with complete head shape outline digitization, the accurate knowledge of the sensor position with respect to the subject head allowed the accurate representation of the reconstructed activity in anatomical space, and correspondingly accurate displays of superimposed functional and anatomical images (Fuchs et al., 1995).

Distributed source analysis

The current density throughout the brain was estimated using the CURRY 4.5 source localization software (Philips Res. Lab.), with a minimum L2-norm constraint for the currents (Hämäläinen and Ilmoniemi, 1994). The source reconstruction was performed using a realistically shaped volume conductor model (BEM, Fuchs et al., 1998), which requires a tessellated representation of the inner and outer skull and scalp surfaces (Fig. 3). The head/brain compart-

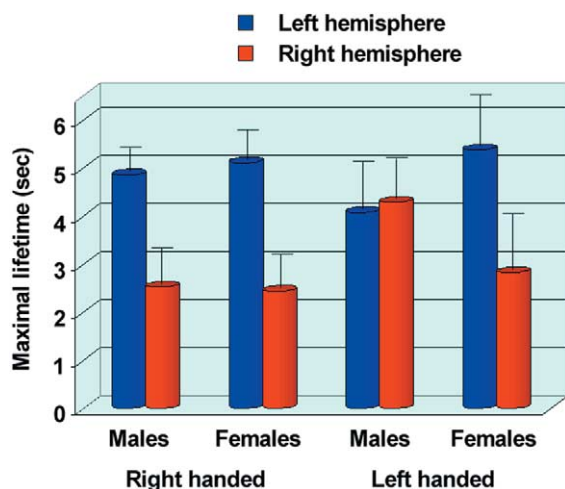


Fig. 7. Interhemispheric comparison of the maximal lifetime values. The right-handed subjects (males and females) show a marked interhemispheric asymmetry, with lifetime values prolonged on the left hemisphere. A shift toward symmetry is clearly noticed in left-handed males, but was not evident in left-handed females. (L) and right hemisphere (R).

ments were semiautomatically segmented from MRI data by a fast 3D region-growing algorithm and then triangulated using a thinning algorithm with different radii (Wagner et al., 1995). The individual in vivo tissue conductivities are not known (Geddes and Baker, 1963), but there is only a very weak dependence on the conductivity ratios of the BEM model compartments used. We thus used the default values from CURRY, 0.33, 0.0042, and 0.33 for the skin, skull, and liquor compartments, respectively. MEG reconstructions using realistic volume conductor models are prone to overemphasizing quasi-radial current components due to their small gain (Menninghaus and Lutkenhoner, 1995). In order to limit this effect, as well as to avoid overfitting the noise in the measured data, the L-curve regularization was performed (Hämäläinen and Ilmoniemi, 1994).

The minimum L2-norm solution was computed at latencies between -100 and 400 ms relative to the stimulus onset. The source space was defined as a regular grid of points distributed in 34 parallel planes equally spaced at 5 mm (the in-plane distance between points was also 5 mm in each direction). The sources were further constrained to be at least 3 mm inside the liquor boundary. A magnetic coil quadrature of 9 points/coil was used in order to improve the accuracy of the forward problem. The source reconstruction was performed using a diagonal location-weighting matrix for depth bias removal.

Results

Identification of non-time-locked activations

For quantitative analysis we computed the output of VS, defined by the weighted sum of a subset of signals selected

at the dominant M100 response. A VS was separately defined for each subject and hemisphere (Fig. 2A). Wavelet analysis was employed to compute the energy in the time-scale or time-frequency plane and hence quantified the level of NTLA. Significant spontaneous NTLA was observed in 16 of 24 subjects on the long silent intervals (8 s), especially on those preceded by long contextual ISIs (5 or 8 s). The NTLA was rarely identified at short ISIs. In some cases the highest NTLA activity was detected after a silent temporal segment equal in duration to the preceding (contextual) ISI, which may be similar in origin to a response to an omitted stimulus, as observed in other MEG studies (Joutsiniemi and Hari, 1989; Rogers et al., 1992; Raji et al., 1997). Fig. 4 shows examples of VS output and their wavelet analysis for the same two segments for two subjects. The first segment contains tones with short ISIs (beginning of run 3 in Fig. 1), with onsets at 0, 1, 3, 5, 6.5, and 7.5 s. The second segment contains the next two stimuli from the same run, with onsets at 12.5 and 20.5 s. The first subject (Fig. 4A) shows no noticeable NTLA in either segment while the second subject (more typical for the group, Fig. 4B) shows clear NTLA in the segment with long ISI. The evoked responses are clear on the averaged block signals as well as on the averaged wavelet scalograms and Z score diagrams for both subjects. The highest NTLA (marked by a heavy arrow) for the second subject is at 18 s, when no stimulus was delivered. The non-time-locked nature of this endogenous activation is confirmed by the low POF values, while the relatively large Z scores provide statistical confirmation for persistent NTLA across single trials. Closer inspection of the single trial VS output reveals that significant NTLA is present either as a well-defined transient response or as a sustained train of alpha oscillations lasting for about 500 ms. It should be stated that the peak of the NTLA energy on the averaged scalograms is always noticed at frequencies where the summation of the spectral energies of the two patterns observed in different single trials is maximal. The time interval between the occurrence of the highest NTLA and the onset of the previous tone is close to the value of the preceding ISI, i.e., 5 s (see run 3 in Fig. 1), which suggests that at least in some of the single trials a response to an “omitted stimulus” is generated. The responses evoked by stimuli were clearly identified for all subjects in frequency bands ranging from 5 to 12 Hz, while the NTLA activity extended in slightly lower frequency range, i.e., from 3 to 10 Hz.

We explored the question of how these second-order activations drive new memory traces and affect the response to the next external stimulus by contrasting the averaged responses from three sets of trials. The first two sets have the same long target ISI, $x = 8$ s, but one has little or no significant NTLA while the other has high NTLA spread around a (virtual) target ISI $\Delta t = 2.75$ s. The third average comes from single trials with the sum of contextual and target ISI close to x , and (true) target ISI close to Δt .

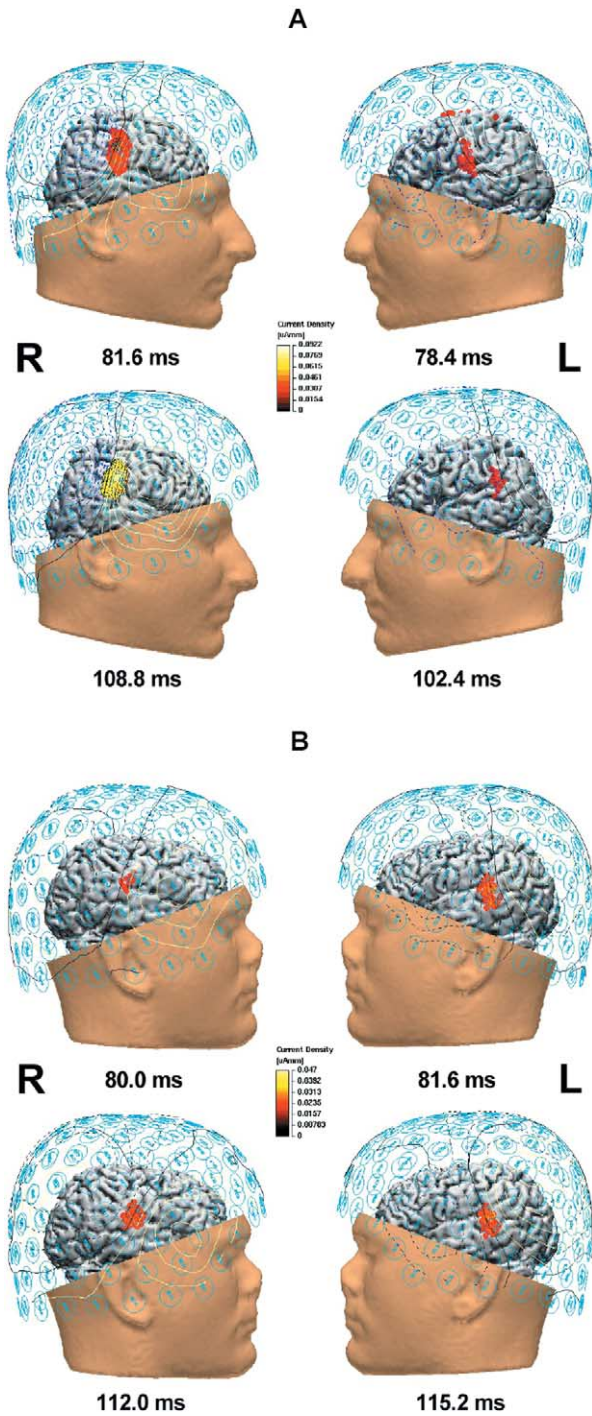


Fig. 8. Comparative evaluation of the current density reconstructions for subjects S2 (right-handed male, A) and S14 (left-handed male, B). The cortical activations are shown in lateral views at early and late latencies around M100 peak. Different columns illustrate the activations in the left (L) and right hemisphere (R).

According to the criteria described in the previous section, for $\Delta t = 2.75$ and $x - \Delta t = 5.25$, two candidate subaveraged signals were available for comparison, i.e., $s_{2|5}$ and $s_{3|5}$. Despite the relatively low SNR afforded by just 30 single trials, all cases in which such a comparison was

possible showed that high NTLA leads to reduction in the average response to the next real external stimulus, as Fig. 5 demonstrates.

Estimation of the EMT lifetime

Fig. 6 illustrates the evoked responses at different ISIs and the fitting parameter τ versus latency for subject S1, left and right auditory cortex, respectively. Around each major positive and negative deflection of the VS signals, the dependence of the activation strength on ISI was well-described by the exponentially saturating function over extended latency segments. In between these latency ranges the responses were close to zero, producing too few average signal values with high SNR at different ISIs to attempt a good fit. The latency dependence of the parameter τ splits into segments that repeat around each peak of the signal. In the left hemisphere lifetime values in each segment increase with latency, while on the right a segment has an inverted “U” shape. Fig. 6E shows the VS data and the corresponding fitting function at two latencies, one at the M100 peak (104 ms) and the other on the descending part of M100 (128

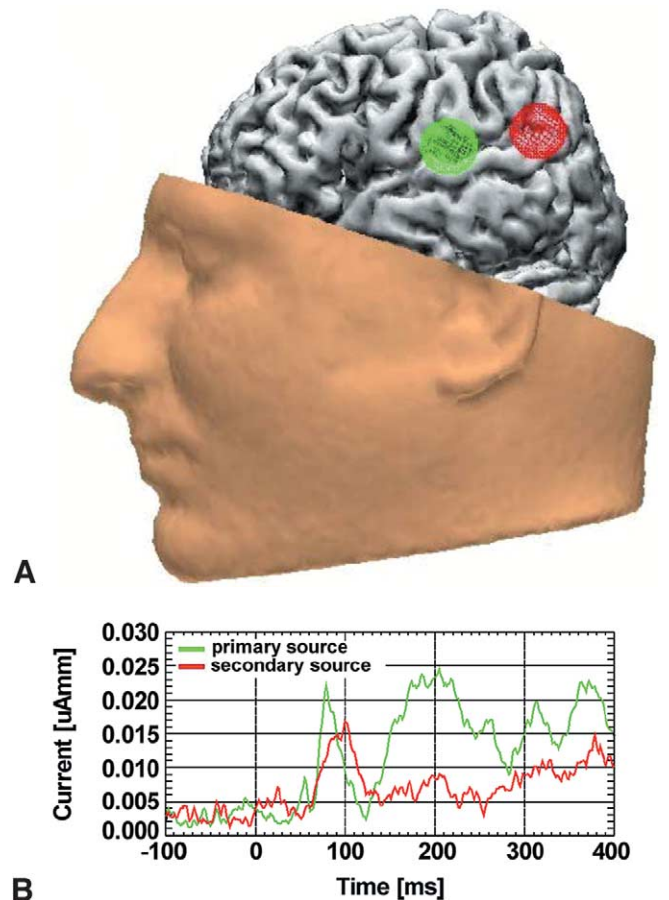


Fig. 9. The VOI definition for the subject S2 (right-handed male), left hemisphere (A), and the corresponding activation curves (B).

ms). The EMT lifetimes at the M100 peak are very similar (1.6 and 1.4 s) on the left and right hemispheres, but very different on the descending part of M100, with much longer decay lifetimes on the left hemisphere (τ values increase up to 5.5 s) than on the right hemisphere (τ values increase up to only 2.2 s).

The results shown in Fig. 6 are broadly representative across subjects at the M100 peak. The maximal τ value (usually on the descending part of M100) varies considerably across subjects with evidence of laterality dependence on gender and handedness. Table 1 summarizes the results of the lifetime estimation (τ) across subjects for the left and right auditory cortex at the mean latency of the M100 peak (denoted by \bar{L}_{M100}) and the maximal values in a time window between 70 and 140 ms. In some cases no acceptable fit was obtained at latency \bar{L}_{M100} , and for the closest latency with a good fit was chosen. For many subjects a fit to the exponentially saturating function could only be obtained after the set with the longest ISI was excluded. For four right-handed subjects (two males), two sets with the longest ISIs (5 and 8 s) had to be excluded. The deterioration of signal quality for the excluded sets of long ISIs was associated with high NTLA activity, which was particularly persistent in the two right-handed females. Strong lifetime asymmetry appears just after the M100 peak latencies. For all right-handed male and all female subjects the descending part of M100 has longer τ values on the left than on the right hemisphere. The left-handed males are the only subjects with comparable maximal τ value on the two hemispheres.

Multiple ANOVAs with appropriate Bonferroni corrections of the significance levels were employed to test the effects of handedness and gender, as well as their possible interaction. Two separate three-way ANOVAs in which the independent variables were handedness, gender, and hemisphere were used to assess the dependence of the lifetime values at M100 peak and of maximal lifetime values, respectively. A significant main effect of hemisphere ($F = 39.58$, $P < 0.001$) and a gender by hemisphere interaction ($F = 7.07$, $P = 0.011$) emerged for the maximal lifetime values. Moreover, the handedness by hemisphere ($F = 5.23$, $P = 0.028$) and the handedness by hemisphere by gender ($F = 4.36$, $P = 0.043$) interactions were close to the corrected significance level. No significant main effects or interactions ($P > 0.05$) were present for lifetimes at \bar{L}_{M100} . A separate two-way ANOVA was also employed in order to test the effects of handedness and gender on the asymmetry coefficients. The asymmetry coefficients show significant main effects of handedness ($F = 9.89$, $P = 0.005$) and gender ($F = 9.72$, $P = 0.005$), as well as a significant handedness by gender interaction ($F = 8.1$, $P = 0.009$). The statistical analysis shows that the EMT lifetime is similar on the left and right hemispheres at the M100 peak latency but, for later latencies, high EMT lifetimes are encountered with laterality that depends on handedness and gender (Fig. 7).

Source localization results

Fig. 8 shows examples of current density reconstruction for subjects S2 (right-handed male) and S14 (left-handed male). The displays show activations on the superficial cortical surface at early and late latencies around the M100 peak for the left and right hemisphere. The activation patterns show that sites in the vicinity of the temporal–parietal junction were typically responsive to the tone stimuli in all subjects, but the precise location and the temporal interplay between their activities depends on hemisphere and handedness. The cortical activation is identified first within the primary auditory cortex (Brodmann area 41) or close by in both hemispheres and extends with latency toward areas of the auditory association cortex, including areas of the posterior temporal–parietal junction, across the supratemporal gyrus and planum temporale (which includes the Wernicke's area of the language dominant hemisphere). Significant activation patterns were consistently observed for about 30 ms around the M100 peak in parietal areas (supramarginal and postcentral gyri) of both hemispheres. The same findings have been reported in a recent study using intracranial recordings of middle-latency responses to auditory stimuli (Hughes et al., 2001). For long latencies (after 130 ms) we noticed the consistent activation of the right hemisphere homologue of the Broca's area (inferior frontal gyrus), which was recently suggested to be involved in processing of the musical syntax (Maess et al., 2001). Particularly, the activation of the posterior part of the superior temporal gyrus and around the posterior end of the Sylvian fissure in the left hemisphere of the right-handed subject reveals a secondary generator which is well-separated in space (by almost 2 cm) from areas encompassing the primary auditory cortex (primary generator). A secondary generator was also present on the right hemisphere of the right-handed male, but it was not as clearly separated in space and time from the primary generator as in the left hemisphere. A clear spatial separation between an early anterior and a late posterior generator was not noticed in either of the two hemispheres of the left-handed male. In order to track the time course of the activation in the primary and secondary generators which were most clearly distinguished in the left hemispheres of the right-handed subject, the modulus of the current density estimate was separately integrated over two spherically shaped volumes of interest (VOIs) defined as shown in Fig. 9A. The time course of the activations of the primary generator and the more posterior generator on the left hemisphere of the right-handed subject were distinct, with the posterior generator peaking later than the primary generator. The corresponding activation curves (Fig. 9B) show that the primary generator peaks at 78 ms, while the secondary generator peaks 25 ms later. The fact that the secondary generator dominates the auditory response at late latencies of M100 (where EMT lifetime asymmetry was actually detected) suggests that it is a candidate source to

explain the interhemispheric asymmetry in the lifetime of the echoic memory for right-handed subjects.

Discussion

Earlier studies explored the properties of the EMT through estimates of the activity in one or two cortical auditory areas. It is very likely that the latency dependence of the echoic memory lifetime is a property of the wider auditory system, which is not limited to either the primary auditory cortex or any one subarea: if synchronization of different oscillatory sources contributes to the compound MEG signal, then this will be missed in a model postulating separate sources. The present study has put the emphasis on the latency dependence, and hence indirectly allowed for the existence of multiple EMTs. Given the clear difference between the left- and right-handed male subjects, we reconstructed the spatiotemporal activations in the brain for one left- and one right-handed male, for which accurate head-shape outlines were available to allow precise superimposition of functional and anatomical data. The reconstructions provided a glimpse of the complexity involved, as demonstrated in Fig. 8, but also provided hints about the generator structure, which might be responsible for the observed laterality and gender effects.

The wavelet analysis revealed NTLA and allowed us to identify its effect (lower amplitude) on the next evoked response. As the quantitative estimation of the EMT lifetimes requires a precise knowledge of the silent time interval between consecutive activations, data strongly influenced by NTLA were treated as deviant and were excluded from the EMT parameter fitting. Different mechanisms may account for the NTLA generation across subjects or even in different single trial signals recorded from the same subject. We have already pointed out the similarity of NTLA to responses to omitted stimuli. NTLA may be related to an attentional switching rhythm with periodicity of about 3 s (Pöppel, 1997). Effortless primitive partitioning and temporal integration are present for intervals of up to 3 s, such as the subjective structuring of continuous auditory streams (Szélag et al., 1996) and temporal segmentation of speech (Vollrath et al., 1992). The NTLA bias for long silent intervals can be explained by assuming that each incoming train of tones used in the present study resets such an attentional switching rhythm. NTLA will then be seen only for long ISIs (5 and 8 s), i.e., when the gap between auditory events exceeds the *universal* time constant of 3 s. This effect was slightly stronger in the left hemisphere, especially on the descending part of M100. The correlation between the NTLA presence on long silent intervals (ISI = 5, 8 s) and the decrease in amplitude of the next response to an external stimulus offers a potential explanation for the dependence of mismatch negativity (MMN) on ISI. Specifically, the MMN elicited by physically deviant stimuli in a homogeneous sequence of standard stimuli (Näätänen, 1990) had amplitude that increased up to only an ISI value of 3 s

(Sams et al., 1993). Moreover, NTLA and its preferential occurrence on long silent segments may also relate to sleepiness, which is known to decrease the auditory evoked response amplitude (Weitzman and Kremer, 1965; Fruhstorfer and Bergstrom, 1969; Wesensten and Badia, 1988) and was previously documented by a reactive ‘tau’ rhythm of the auditory cortex (Lehtelä et al., 1997). The design of our experiment, however, does not allow us to distinguish between the mechanisms of NTLA generation listed above.

The key finding of our work is the evidence of hemispheric lateralization for EMT with long lifetimes, which depends on gender and handedness. The interhemispheric asymmetry of the EMT lifetime was not evident at the signal peaks, and this may explain why previous studies failed to detect it. The increase in the EMT lifetime at long latencies is due to a higher dispersion of the signal amplitude on the descending part of the M100 for different ISIs (Fig. 6). This is consistent with the published data from other laboratories, as seen in Fig. 3 of Mäkelä et al. (1993). However, the absence of handedness and gender effects in the Mäkelä et al. study cannot be discussed since no information was provided about the handedness of the subjects, and the results from males and females were pooled together.

Although left hemisphere language dominance has been well-documented, the underlying physiological basis of speech and language processing remains a major challenge for cognitive neuroscience, as most aspects are still obscure or under debate. Compared to the great number of recent studies on speech perception, little work has been done on assessing the echoic memory and its possible implication in the subsequent processing of speech by the human brain. The echoic memory is essential for integrating the successive neuronal imprints and grouping the perceptual features whenever acoustic information (particularly speech or melodic signals) is continuously presented. The present study shows that the left hemisphere is characterized by significantly higher lifetimes of the memory traces in dextrals (males and females), which suggests that the echoic memory may play a genuine role in the different subsequent perceptual analysis of the input acoustical streams in the two hemispheres. While each hemisphere appears capable of constructing sound-based representations of heard speech, these processing streams may be differentially modulated by the longer lasting memory traces in the left auditory cortex. Larger decaying lifetimes imply sustained prolonged firing that may reflect a higher degree of lateral connections in the left hemisphere. Asymmetry in anatomy between left and right auditory areas in dextrals includes differences in the layout of the intrinsic connections and microcircuitry organization (Galuske et al., 2000), which could sustain prolonged firing and hence longer EMT lifetimes. Temporal information coding and its left hemisphere advantage may be founded on these persistent activations which augment cellular mechanisms for neural delays such as inhibitory post-synaptic potentials and rebound excitations (Jaffe, 1992), or intrinsic oscillations (Miall, 1989).

The proposal that association connections on the left hemisphere include a higher proportion of slow axons than those on the right hemisphere may also offer the biological basis of the cerebral asymmetry in the persistence of the neural trace established by an acoustical event (Miller, 1996). Meaningful processing of acoustic signals requires neural delay lines (Bankes and Margoliash, 1993), which allow the coupling of activations induced by a current acoustical event with the delayed responses from preceding events. Delay lines have been suggested to be crucial for representing temporal patterns. A neuronal network that has the capacity to integrate a large repertoire of brief acoustical events (which may occur in spoken language, for example) would need a correspondingly rich repertoire of delay lines. Thus, an alternative interpretation of the larger maximal lifetime values on the left hemisphere, which was noticed in all right-handed subjects and in the left-handed females, consists of a higher dispersion of the lifetimes, as exemplified in Fig. 6.

Gender differences in brain function lateralization and especially the study of gender–laterality interaction has been controversial because of the large variability of observables within a given gender and handedness group (Spinger and Deutsch, 1989). Greater deficits in visuospatial tasks after right hemisphere temporal lobe removal and greater deficits in verbal tasks after left temporal lobe removal were identified only in males (Lansdell, 1962). An intriguing similarity was observed in cerebral blood flow for male and female right-handed subjects (Gur et al., 1982), while in a separate study, anatomical asymmetry of the human motor cortex was associated with handedness in males but not in females (Amunts et al., 2000). The testosterone hypothesis offers a speculative, but all-embracing, solution to the lateralization–gender findings and links many earlier studies in diverse fields, from behavioral deficits of the body's immune system to a range of disorders like dyslexia (Geschwind and Galaburda, 1987). The evidence for gender–laterality dependence reported in our study was drawn from MEG data with a modest number of subjects; verification of these results with more subjects as well as identification of behavioral correlates of the EMT lifetime and its asymmetry will be addressed in future studies. Our results nevertheless show that probing the latency dependence of the EMT with MEG may be a very sensitive tool for studying mechanisms governing perception of subtle differences in the timing of acoustic speech transients, which may contribute to understanding changes following aging (Sommers, 1997) and failure in aphasia.

Acknowledgments

One of the authors (M.P.) was supported by the General Secretariat for Research and Technology (GSRT) of Greece, Program PENED (ED146) in the first half of this project.

References

- Amunts, K., Jäncke, L., Mohlberg, H., Steinmetz, H., Zilles, K., 2000. Interhemispheric asymmetry of the human motor cortex related to handedness and gender. *Neuropsychologia* 38 (3), 304–312.
- Bankes, S.C., Margoliash, D., 1993. Parametric modeling of the temporal dynamics of neuronal responses using connectionist architectures. *J. Neurophysiol.* 69, 980–990.
- Boatman, D., Hart, J., Lesser, R.P., Honeycutt, N., Anderson, N.B., Miglioretti, D., Gordon, B., 1998. Right hemisphere speech perception revealed by amobarbital injection and electrical interference. *Neurology* 51, 458–464.
- Bugmann, G., 1997. Biologically plausible neural computation. *BioSystems* 40, 11–19.
- Bugmann, G., Taylor, J.G., 1997. A stochastic short-term memory using a pRAM neuron and its potential applications, in: Beale, R., Plumbey, M.D. (Eds.), *Recent Advances in Neural Networks*, Ellis Horwood Publishing, UK.
- Celesia, G.G., 1976. Organization of auditory cortical areas in man. *Brain* 99, 403–414.
- Corballis, M.C., 1998. Cerebral asymmetry: motoring on. *Trends Cogn. Sci.* 2 (4), 152–158.
- Creutzfeldt, O., Ojemann, G., Lettich, E., 1989. Neuronal activity in the human lateral temporal lobe. I. Responses to speech. *Exp. Brain Res.* 77, 451–475.
- Fruhstorfer, H., Bergstrom, R., 1969. Human vigilance and auditory evoked responses. *Electroenceph. Clin. Neurophysiol.* 27, 346–355.
- Fuchs, M., Wischmann, H.A., Wagner, M., Kruger, J., 1995. Coordinate system matching for neuromagnetic and morphological reconstruction overlay. *IEEE Trans. Biomed. Eng.* 42, 416–420.
- Fuchs, M., Drenckhahn, R., Wischmann, H.A., Wagner, M., 1998. An improved boundary element method for realistic volume-conductor modeling. *IEEE Trans. Biomed. Eng.* 45, 980–997.
- Galuske, R.A.W., Schlote, W., Bratzke, H., Singer, W., 2000. Interhemispheric asymmetries of the modular structure in human temporal cortex. *Science* 289, 1946–1949.
- Geddes, L.A., Baker, L.E., 1963. The specific resistance of biological material, a compendium of data for the biomedical engineer and physiologist. *Med. Biol. Eng. Comput.* 5, 271–293.
- Geschwind, N., Galaburda, N., 1987. *Cerebral Lateralization: Biological Mechanisms, Associations and Pathology*. MIT Press, Cambridge, MA.
- Grossberg, S., Merrill, J.W.L., 1992. A neural model of adaptively timed reinforcement learning and hippocampal dynamics. *Cogn. Brain Res.* 1, 3–38.
- Grossberg, S., Merrill, J.W.L., 1996. The hippocampus and cerebellum in adaptively timed learning: recognition and movement. *J. Cogn. Neurosci.* 8 (3), 257–277.
- Gur, R.C., Gur, R.E., Obrist, W.D., Hungerbuhler, J.P., Younkin, D., Rosen, A.D., Skolnick, B.E., Reivich, M., 1982. Sex and handedness differences in cerebral blood flow during rest and cognitive activity. *Science* 217, 659–661.
- Hämäläinen, M.S., Ilmoniemi, R.J., 1994. Interpreting magnetic fields of the brain: minimum norm estimates. *Med. Biol. Eng. Comput.* 32, 35–42.
- Hari, R., Katila, K., Tuomisto, T., Varpula, T., 1982. Interstimulus interval dependence of the auditory vertex response and its magnetic counterpart: implications for their neural generation. *Electroenceph. Clin. Neurophysiol.* 54, 561–569.
- Hari, R., Pelizzone, M., Mäkelä, J.P., Hällström, J., Leinonen, L., Lounasmaa, O.V., 1987. Neuromagnetic responses of the human auditory cortex to on- and offsets of noise bursts. *Audiology* 26, 31–43.
- Hickok, G., Poeppel, D., 2000. Towards a functional neuroanatomy of speech perception. *Trends Cogn. Sci.* 4, 131–138.
- Hughes, H.C., Darcey, T.M., Barkan, H.I., Williamson, P.D., Roberts, D.W., Aslin, C.H., 2001. Responses of human auditory association

- cortex to the omission of an expected acoustic event. *NeuroImage* 13 (6), 1073–1089.
- Jaffe, S., 1992. A neuronal model for variable response latency, in: Eeckman, F.H. (Ed.), *Analysis and Modeling of Neural Systems*, Kluwer, Boston, pp. 405–410.
- Jervis, B.W., Nichols, M.J., Johnsson, T.E., Allen, E., Hudson, N.R., 1983. A fundamental investigation of the composition of auditory evoked potentials. *IEEE Trans. Biomed. Eng.* 30, 43–50.
- Joutsiniemi, S.L., Hari, R., 1989. Omission of auditory stimuli may activate frontal cortex. *Eur. J. Neurosci.* 1, 524–528.
- Lansdell, H., 1962. A sex difference in effect of temporal lobe neurosurgery on design preference. *Nature* 194, 852–854.
- Lehtelä, L., Salmelin, R., Hari, R., 1997. Evidence for reactive magnetic 10-Hz rhythm in the human auditory cortex. *Neurosci. Lett.* 222, 111–114.
- Liegeois-Chauvel, C., de Graaf, J.B., Laguitton, V., Chauvel, P., 1999. Specialization of left auditory cortex for speech perception in man depends on temporal coding. *Cereb. Cortex* 9, 484–496.
- Liu, L.C., Ioannides, A.A., Taylor, J.G., 1998a. Observation of quantization effects in human auditory cortex. *Neuroreport* 9, 2679–2690.
- Liu, L.C., Ioannides, A.A., Müller-Gärtner, H.W., 1998b. Bi-hemispheric study of single trial MEG signals of the human auditory cortex. *EEG Clin. Neurophysiol.* 106, 64–78.
- Lü, Z.L., Williamson, S.J., Kaufman, L., 1992a. Human auditory primary and association cortex have different lifetimes for activation traces. *Brain Res.* 572, 236–241.
- Lü, Z.L., Williamson, S.J., Kaufman, L., 1992b. Behavioral lifetime of human auditory sensory memory predicted by physiological measures. *Science* 258, 1668–1670.
- Luria, A.R., 1970. *Traumatic Aphasia*. Mouton, The Hague.
- Maess, B., Koelsch, S., Gunter, T.C., Friederici, A.D., 2001. Musical syntax is processed in Broca's area: an MEG study. *Nature Neurosci.* 4, 540–545.
- Mäkelä, J.P., Ahonen, A., Hämäläinen, M., Hari, R., Ilmoniemi, R., Kajola, M., Knuutila, J., Lounasmaa, O.V., McEvoy, L., Salmelin, R., Salonen, O., Sams, M., Simola, J., Tesche, C., Vasama, J.P., 1993. Functional differences between auditory cortices of the two hemispheres revealed by whole-head neuromagnetic recordings. *Hum. Brain Mapp.* 1, 48–56.
- McGlone, J., 1984. Speech comprehension after unilateral injection of sodium amytal. *Brain Lang.* 22, 150–157.
- Menninghaus, E., Lütkenhöner, B., 1995. How silent are deep and radial sources in neuromagnetic measurements? in: Baumgartner, C., Deecke, L., Stroink, G., Williamson, S.J. (Eds.), *Biomagnetism: Fundamental Research and Clinical Applications*, Elsevier, Vienna, Austria, pp. 352–356.
- Miall, C., 1989. The storage of time-intervals using oscillating neurons. *Neural Comput.* 1, 359–371.
- Miller, R., 1996. *Axonal Conduction Time and Human Cerebral Laterality: A Psychobiological Theory*. Harwood Academic Publisher, The Netherlands.
- Näätänen, R., 1990. The role of attention in auditory information processing as revealed by event-related potentials and other brain measures of cognitive function. *Behav. Brain Sci.* 13, 201–233.
- Oldfield, R.C., 1971. The assessment and analysis of handedness: the Edinburgh inventory. *Neuropsychologia* 9, 97–113.
- Pöppel, E., 1997. A hierarchical model of temporal perception. *Trends Cogn. Sci.* 1, 56–61.
- Raij, T., McEvoy, L., Mäkelä, J.P., Hari, R., 1997. Human auditory cortex is activated by omission of auditory stimuli. *Brain Res.* 745, 134–143.
- Rasmussen, T., Milner, B., 1977. The role of early left-brain injury in determining lateralization of cerebral speech function. *Ann. NY Acad. Sci.* 299, 355–369.
- Ringo, J.L., Doty, R.W., Demeter, S., Simard, P.Y., 1994. Time is of the essence: a conjecture that hemispheric specialization arises from inter-hemispheric conduction delay. *Cereb. Cortex* 4, 331–343.
- Robin, D.A., Tranel, D., Damasio, H., 1990. Auditory perception of temporal and spectral events in patients with focal left and right cerebral lesions. *Brain Lang.* 39, 539–555.
- Rogers, R.L., Papanicolaou, A.C., Baumann, S.B., Eisenberg, H.M., 1992. Late magnetic fields and positive evoked potentials following infrequent and unpredictable omission of visual stimuli. *Electroenceph. Clin. Neurophysiol.* 83, 146–152.
- Sams, M., Hari, R., Rif, J., Knuutila, A., 1993. The human auditory sensory memory trace persists about 10 sec: neuromagnetic evidence. *J. Cogn. Neurosci.* 5, 363–370.
- Sommers, M.J., 1997. Speech perception in older adults: the importance of speech-specific cognitive abilities. *J. Am. Geriatr. Soc.* 45, 633–637.
- Spinger, S.P., Deutsch, G., 1989. *Left Brain, Right Brain*. Freeman, New York.
- Szelag, E., Steinbüchel, v N., Reisen, M., de Langen, E., Pöppel, E., 1996. Temporal constraint in processing of nonverbal rhythmic patterns. *Acta Neurobiol. Experimentalis* 56, 215–225.
- Tallon-Baudry, C., Bertrand, O., Peronnet, F., Pernier, J., 1998. Induced γ -band activity during the delay of a visual short-term memory task in humans. *J. Neurosci.* 18, 4244–4254.
- Vetterli, M., 1995. *Wavelets and Subband Coding*. Prentice Hall PTR, Englewood Cliffs, NJ.
- Vollrath, M., Kazenwadel, J., Krüger, H.P., 1992. A universal constant in temporal segmentation of human speech—a reply to Schleidt & Feldhutter (1989). *Naturwissenschaften* 79, 479–480.
- Wagner, M., Fuchs, M., Wischmann, H.A., Ottenberg, K., Dössel, O., 1995. Cortex segmentation from 3-D MR images for MEG reconstructions, in: Baumgartner, C., Deecke, L., Stroink, G., Williamson, S.J. (Eds.), *Biomagnetism: Fundamental Research and Clinical Applications*, Elsevier Science, Vienna, Austria, pp. 352–356.
- Wearden, J.H., 1992. Temporal generalization in humans. *J. Exp. Psychol. Anim. Behav. Process* 18, 134–144.
- Weitzman, E.D., Kremer, H., 1965. Auditory evoked responses during different stages of sleep in man. *Electroenceph. Clin. Neurophysiol.* 18, 65–70.
- Wernicke, C., 1977. in: Eggert, G.H. (Ed.), *Wernicke's Works on Aphasia: A Sourcebook and Review*. Mouton, The Hague, pp. 91–145.
- Wesensten, N.J., Badia, P., 1988. The P300 component in sleep. *Physiol. Behav.* 44, 215–220.
- Zaidel, E., 1985. in: Benson, D.F., Zaidel, E. (Eds.), *The Dual Brain: Hemispheric Specialization in Humans*, Guilford Press, pp. 205–231.